Research on Engineering Structures & Materials
www.jresm.org
Research Group

Research Article

Numerical investigation into the axial performance of single and double skin CFST Columns: Influence of shear stud spacing and tube thickness

Bashar F. Abdulkareem [*,1,a], Mustafa Musa Salih [1,b], Raid I. Khalel [2,c], Nameer N. Salman [3,d], Nooralmustafa Ali [3,e], Mahdi Karkush [1,f]

[1]*Reconstruction and Projects Department, University of Baghdad, Baghdad, Iraq*
[2]*College of Civil Engineering, University of Technology, Baghdad, Iraq*
[3]*College of Engineering, Al-Nahrain University, Baghdad, Iraq*

Article Info

Article History:

Received 01 Sep 2026
Accepted 03 Nov 2026

Keywords:

ABAQUS;
CFST columns;
Shear connectors;
Axial loading;
Double-skin CFST;
Shear strength;
Parametric study

Abstract

This research presents the results of a finite element (FE) simulation conducted with the ABAQUS/CAE software. The goal of the project was to develop a simulation model that can predict the structural behavior of CFST columns (single or double skin) and studying the effect of shear stud spacing in double-skin columns. Findings were evaluated in comparison with documented experimental data in the existing literature (Younes et al., 2015). FE approach and the experimental data were in agreement with an average error of 2.4%; hence, the simulated model was deemed valid. Subsequently, the scope of numerical studies was expanded to encompass the examination of several factors, including the concrete skin type, the outer steel tube thickness, and the vertical spacing of studs. the capacity of double-skin columns was found to be between 4.8% and 6.6% higher than their single-skin counterparts. This may result from the selected dimensions of the samples and the inclusion of the internal steel tube, which enhances the column's load-bearing capability. Reducing the vertical spacing of shear connectors leads to an increase in ultimate strength of 8.9% and 13.8% for single skin columns with spacings of 100 mm and 50 mm, respectively, in comparison to the single skin column with a spacing of 200 mm, and by 10.7% and 13.5% for double skin columns with spacings of 100 mm and 50 mm, respectively, when compared to the double skin column with a spacing of 200 mm. The vertical spacing of shear connections is inversely related to the ultimate load of the column.

© 2026 MIM Research Group. All rights reserved.

1. Introduction

Concrete-Filled steel tube (CFST) columns amalgamate steel and concrete to improve structural performance. They offer significant load-bearing strength, reduced column dimensions, enhanced ductility, and greater seismic resistance. The external steel tube acts as permanent formwork, expediting construction and protecting the concrete core from spalling and environmental deterioration. The concrete core primarily provides significant compressive load-bearing strength and serves as an internal support [1-3].

In Concrete-Filled Steel Tube (CFST) columns, shear connectors such as shear studs, steel bars, or plates primarily function to physically bond the external steel tube with the inside concrete core. They prevent separation, diminish relative slippage, and ensure that the two materials operate as a unified composite entity. Also, the shear connectors play an important role in load transfer between the inner and outer tubes [4-6].

*Corresponding author: b.faisal1101@coeng.uobaghdad.edu.iq
[a]orcid.org/0000-0001-7038-9857; [b]orcid.org/0000-0002-3454-4677; [c]orcid.org/ 0000-0003-4182-2046; [d]orcid.org/0009-0006-0818-5291; [e]orcid.org/ 0009-0005-2811-7811; [f]orcid.org/0000-0003-1304-0303
DOI: http://dx.doi.org/10.17515/resm2026-2094st0801rs

1.1 Single-Walled CFSTs

Almamoori [7] reported the results of an experimental study investigating the behavior of 19 lightweight concrete CFST columns subjected to axial loads. The CFST columns exhibited diverse cross-sectional shapes to evaluate the optimal arrangement for confinement and stability. All components were engineered to have approximately equal area and perimeter. The results reveal that the octagonal CFST columns exhibited the greatest failure load. As the shape becomes increasingly irregular, its ductility index decreases. A numerical model was developed using ABAQUS by [8], and its accuracy was validated through correspondence with conventional damage methodologies and loads observed during testing. The axial performance of precast circular continuous concrete-filled tube (PCCFT) columns was studied. A case study was conducted to investigate the influence of yield strength, the diameter-to-thickness ratio, slenderness ratio, and additional parameters on the axial performance of PCCFT columns. Fluctuations in yield strength, slenderness ratio, and the diameter-to-thickness ratio of the upper and lower steel tubes considerably affect the specimen's load-bearing capacity, while changes in stud diameter and the outer tube's diameter-thickness ratio have a negligible effect on bearing strength.

To swiftly and effectively improve CFST columns, two methods, fibre reinforced polymer (FRP) and steel strips, were examined by [9]. Two unreinforced CFST columns, eight specimens reinforced with FRP, and four specimens reinforced with manufactured steel strips were constructed and assessed. The results demonstrate that the strength of CFST columns increased by 28.7 to 64.1% after being confined with FRP, utilizing one to four layers. The peak load of the constructed steel strips-reinforced CFST column, utilizing 0.3 and 0.6 cm steel strips, increased by 28.5% and 49.8%, respectively, when contrasted with the unreinforced CFST column.

1.2 Double-Walled CFSTs

Experiments were conducted by [10] on 31 concrete-filled double skin tube (CFDST) columns. The CFDST columns experienced axial forces until failure ensued. The parameters that were altered included the diameters, lengths, and tensile strength of the outside steel tubes. The CFDSTs, which are 1 metre long, malfunctioned due to the deformation of the external tubes. All other CFDSTs collapsed due to complete buckling caused by their excessive slenderness. The compressive strength of the CFDSTs decreased as the column lengths increased. He et al. [11] described a set of experiments on the axial compression of steel tubes filled with concrete and double inner circular steel tubes (DIC-CFST) stub columns. The experiments were conducted on 27 specimens with different eccentricity ratios (e), hollow ratios, and concrete strengths. The findings show that both the inner and outer steel tubes exhibit observable local buckling failures under axial compression. Circumferential crushing zones and vertical fractures are signs of concrete collapse. The specimens' load-deformation curve is nearly identical to that of a steel tube filled with concrete in its entirety.

1.3 CFSTs With Shear Connectors

Qiao et al. [12] performed an investigation on shear connectors (steel rings) within square CFST. A finite element method analysis of the steel rings in the CFST was performed to compare with the experimental results. The parameters encompassed the B/t ratio of the tube, the number of steel rings, the thickness of the steel rings, and the spacing between the steel rings. The analytical outcomes correspond closely with the experimental results, and the influence of the separation between two steel rings and the thickness of the rings was investigated. The findings indicate that the thickness of the steel rings influences the specimens' strength; but, above a specific limit, it ceases to affect compressive strength. To quantitatively assess the shear-bearing capability of shear connections in square concrete filled steel tubes (CFST), push-out tests were conducted on 14 square CFSTs equipped with shear connectors by [13]. Of the 14 CFSTs, 13 specimens include steel plate connections, while one example has steel bar connectors. The subsequent factors are examined to determine their effects on the performance of CFSTs: the width-to-thickness ratio of the steel tube, the thickness of the steel plate, the length of the steel plate, the strength of the concrete, the welding conditions of the steel plate, the quantity of plate layers, and the spacing. The findings indicate that the ultimate load and stiffness enhance when the width-to-thickness ratio of the outer tube diminishes, alongside a rise in the thickness and length of the steel plate.

Sarir [14] used finite element analysis using iterative methods to model circular and square concrete-filled steel tube specimens, which were reinforced with a plate along the columns and divided into four equal segments, with variations including both perforated and non-perforated designs. The findings indicated that the plate improved the failure load of both square and circular columns; nevertheless, the structural performance of the square CFST columns was modified, with local buckling observed following the plate's installation. Zhang et al. [15] presented a novel longitudinal-plate shear connection to enhance the interaction shear strength of CFST columns. For this push-out examination, a reference specimen, eight CFST samples including longitudinal-plate shear connections, and a control specimen were all fabricated. The test variables included the number of shear connections, the characteristics of the shear connectors (including thickness, width, and the existence of openings), and the boundary conditions of the longitudinal-plate shear. The results demonstrated that longitudinal-plate shear connectors improved shear strength by up to 725% compared to the control specimen.

Habib et al., [16] conducted an experimental study on the structural performance of CFST utilizing bolt-coupler baseplate (BCB) connections. The BCB connection is an innovative method that optimizes the construction process and reduces costs. Experimental investigations were conducted on 10 specimens (5 short and 5 slender columns) to evaluate the effectiveness of BCB connections in CFST columns for load transmission from the upper column to the lower column. Four CFST columns were constructed without connections, and six specimens were produced with BCB connectors. The findings demonstrated that CFST short columns including BCB connections achieved a load-bearing capacity comparable to or slightly exceeding (about 1.4%) that of CFST columns without connectors. For CFST slender columns including BCB connections, the 87% increase in height compared to short columns resulted in a slight decrease in failure load (about 1.5%) when contrasted with CFST columns without connections.

2. Research Significance

The goal of the project was to develop a simulation model by Abaqus software that can predict the structural behavior of CFST columns (single or double skin) and provide a reliable tool for parametric analyses in cases where physical tests cannot be conducted (due to cost/time constraints) and to study the effect of shear stud spacing and thickness of outer tube in CFST columns. Also, a comparison between single and double skin CFST columns. One of the main advantages of CFST columns is their use in high-rise buildings and bridge piers.

3. Experimental Database for Model Validation

The experimental program from Younes, et al., [17] included testing three CFST columns (with and without shear connectors) subjected to axial loads applied on the concrete and the outer tube. All CFST columns include outer diameter of outer tube = 114.3 mm, with a height of 600 mm, while the thickness was 4 mm. Studs with smooth surface were used as shear connectors with 0.95 cm in diameter and 1.343 cm in length. Figure 1 illustrates the details of the assessed CFST columns. The average cube strength after 28 days was 43.3MPa. Table 1 presents the properties of the steel tube and bolts.

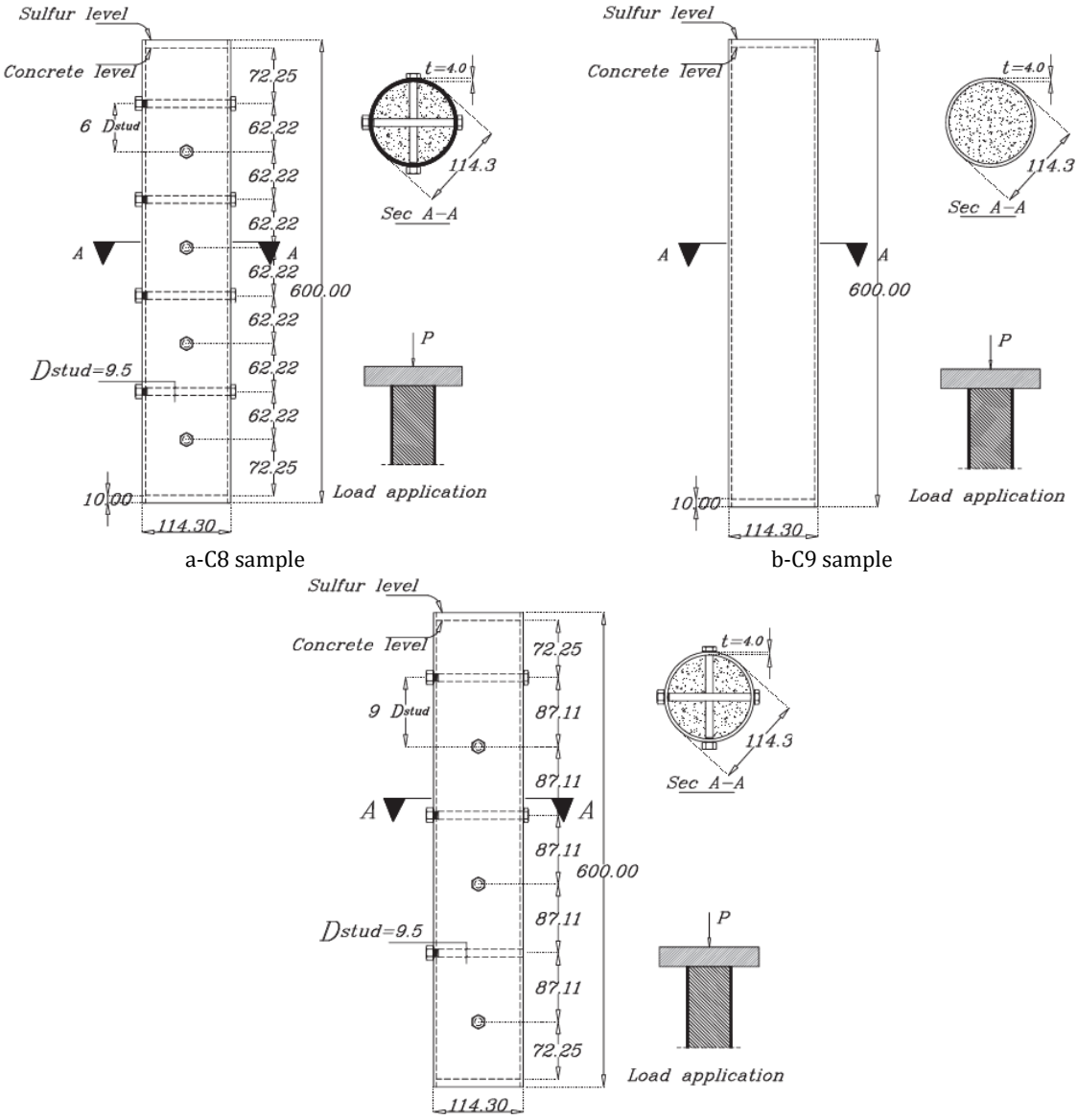
Table 1. Properties of the steel tube and bolts [17]

Material	Elongation percentage (%)	Fy (MPa)	Fu (MPa)	Es (MPa)
Steel	11.2	442.8	508	212000
M10 Bolts	10.8	768.6	791.3	210200

4. Modelling and Analyses of CFST Columns

This investigation uses the Finite Element Technique to examine CFST columns with ABAQUS CAE standard 2022 program, specifically the Standard Model [18]. The isoparametric eight-node brick element (C3D8R) was used to depict the concrete core, load plate, outer steel tube, and bolts. Parts creation is the process of creating specific parts by drawing their shape, such as bolts, concrete, and

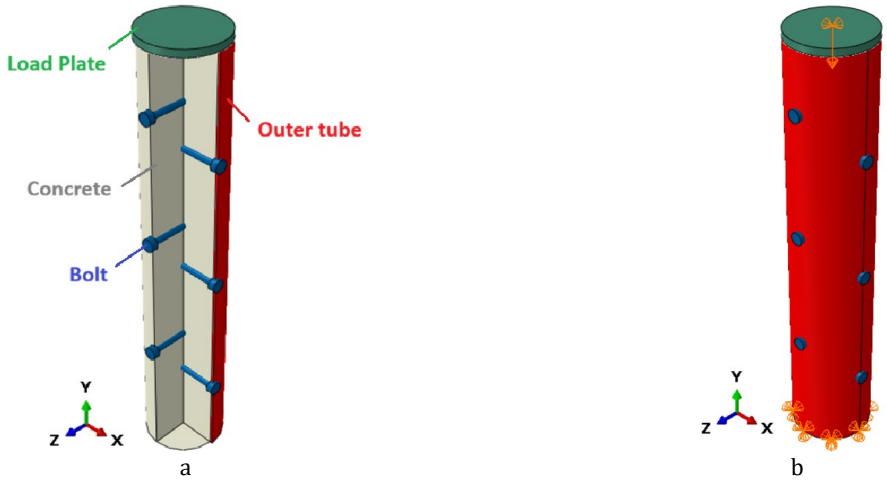
steel tubes, as shown in Figure 2-a. Several pieces were created in order to finish all specimens in the ABAQUS environment. Figure 2-b shows the restrictions of boundary and load parameters.



a-C8 sample b-C9 sample

c-C10 sample

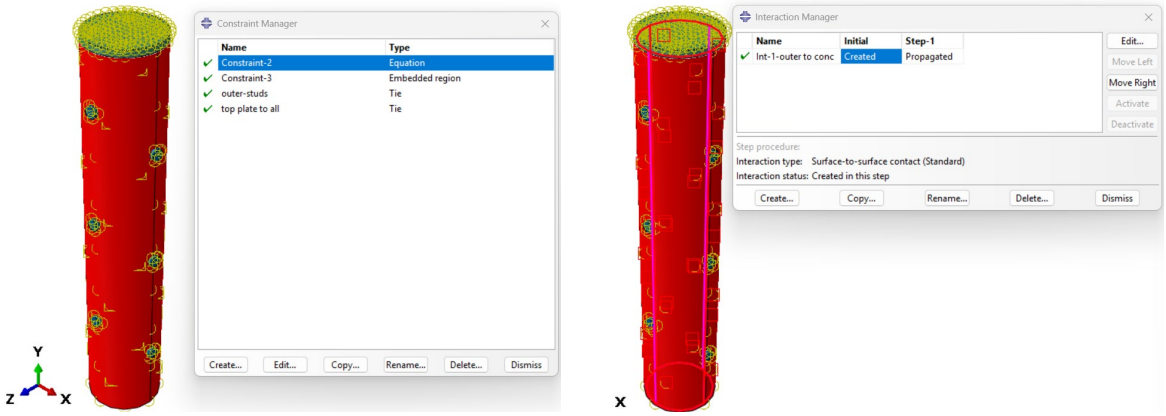
Fig. 1. Details of adopted CFST columns [17]



a b

Fig. 2. a-Creating parts and assemblies, b- boundary and load parameters

For a comprehensive assessment of interaction, the bolts are regarded as entirely embedded in concrete (This method was used to facilitate its representation, despite its limitations). A Tie-type interaction restriction was established between the concrete component and the plates of load. An interaction with contact interaction property which contains two features (Normal behavior with hard contact and tangential behavior with friction coefficient of 0.5) was used for joining two different surfaces together between the concrete and the outer steel tube. A Tie-type interaction limitation was established between the bolts and the outer tube, as seen in Figure 3. Table 2 illustrates the inputs information for damage plasticity of concrete. Table 3 displays the compressive and tensile findings for concrete, computed according to [19] based on the values of fc' (fc'=0.8*43.3=34.64 MPa) according to (BS EN 206:2013+A1:2016) and fct from [17]. The characteristics of the outer tube and bolts are defined as mentioned above in Table 1.



a-Constraints used in this model

b-Interaction between outer tube and concrete

Fig. 3. Interaction of the components

Table 2. Inputs details for damage plasticity of concrete

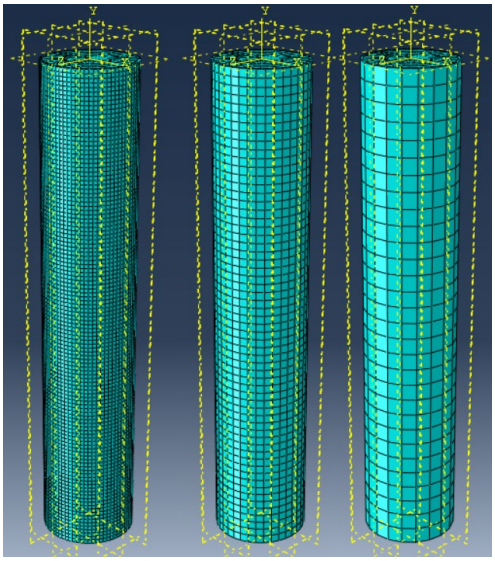
Elasticity modulus (MPa)	Poisson' ratio	Dilation angle (degree)	Eccentricity	ϵ_{bo} /ϵ_{co}	Viscosity
27662	0.17	38	0.1	1.16	0.0009

Table 3. Concrete compressive and tensile information

Compressive information		Tensile information	
Yield-Stress (MPa)	Inelastic strain	Yield-Stress (MPa)	Strain
13.8344	0	3.269764	0
20.0832	2.225E-05	1.989900	0.000145
25.5238	7.740E-05	1.468111	0.000264
29.7213	0.000176	0.860923	0.000585
32.5606	0.0003207	0.626836	0.000893
34.1622	0.0005146	0.442435	0.001400
34.64	0.000747	0.347375	0.001903
33.2573	0.0012927	0.288566	0.002405
30.1665	0.0019084	0.248255	0.002907
26.6316	0.0025372	0.218735	0.003408
23.2825	0.0031533	0.196092	0.003909
20.2503	0.0037669	0.101533	0.008912
17.6615	0.0043615	0.071111	0.013913
9.67501	0.0071252	0.055627	0.018914
5.94433	0.0097801	0.046110	0.023914
4.01189	0.0123549	0.039613	0.028914
2.89615	0.0148703	0.034868	0.033914
2.17742	0.0174162	0.031235	0.038915
1.69865	0.0199385	-	-

4.2 Mesh Sensitivity

A mesh sensitivity study was conducted using three sizes (5, 10, and 20mm) with an aspect ratio of 1, as shown in Figure 4. Figure 5 shows that the curve closest to the experimental results curve is the 10 mm model curve. Therefore, it was adopted.



a-5 mm b-10 mm c-20 mm

Fig. 4. Numerical meshed models

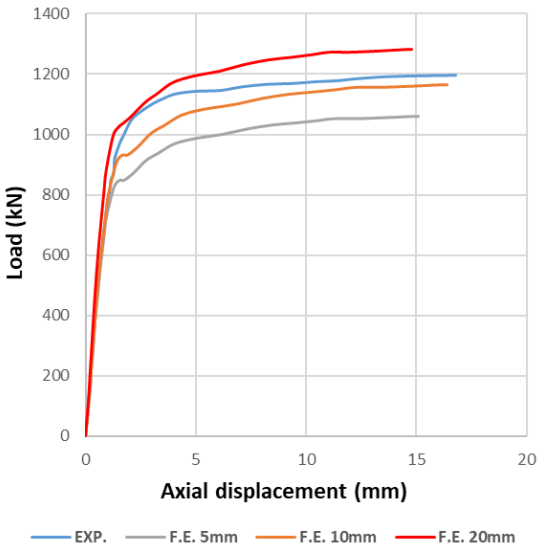


Fig. 5. Mesh sensitivity study

5. Validation of the Developed FE Model

This part presents multiple comparisons between the experimental findings and pertinent numerical results. The areas of focus encompass the relationship between load and axial displacement, as well as the evaluation of load and axial displacement at the failure stage. The experimental results were taken from [17].

5.1 Load vs. Axial Displacement Curves

Figure 6 presents a comparison of the load versus axial displacement relationships obtained from the numerical simulations and experimental tests. The FE models exhibited similar initial stiffness to the experimental curves in the elastic (linear) range. However, in the nonlinear range, the FE models showed slightly lower stiffness and ultimate capacity, although an overall satisfactory agreement was achieved. The finite element models slightly underestimate the load-carrying capacity compared with the experimental results after entering the plasticity region. This may be due to the assumptions regarding concrete damage parameters, the friction model at the steel-concrete interface, or idealizations in the boundary conditions.

5.2 Load and Axial Displacement at Failure

For each sample, Table 4 compares the numerical model's predicted ultimate load and axial displacement to experimental data taken at the failure stage. Results from experiments and finite element models showed a high degree of agreement when it came to the ultimate load and axial displacement, with the mean and coefficient of variation of (Pu) FE/(Pu) EXP being 0.976 and 0.54%, respectively, for failure loads, whereas for axial displacement (Δu FE / Δu EXP) they were 0.975 and 1.36%, respectively.

5.3 Failure Mode at the Ultimate Stage

Figure 7 shows a contour plot of the principal plastic strain in the analyzed numerical columns at the ultimate stage and failure mode of the experimental columns at the ultimate stage. There seems to be some degree of agreement between the two cases. Figure 8 shows the stress distribution in CFST components in (MPa).

Table 4. Ultimate load and axial displacement from experimental and numerical analyses

Column ID	Failure Load (Pu)			Axial disp. at failure load (Δu)		
	EXP. (kN)	FE. (kN)	FE /EXP	EXP. (mm)	FE. (mm)	FE /EXP
C8	1196	1165.1	0.974	16.79	16.41	0.977
C9	1136	1104.2	0.972	12.644	12.16	0.962
C10	1161	1140.1	0.982	12.449	12.3012	0.988
Average			0.976	Average		0.975
Standard deviation			0.011	Standard deviation		0.013
Coefficient of variation (%)			0.54	Coefficient of variation (%)		1.36

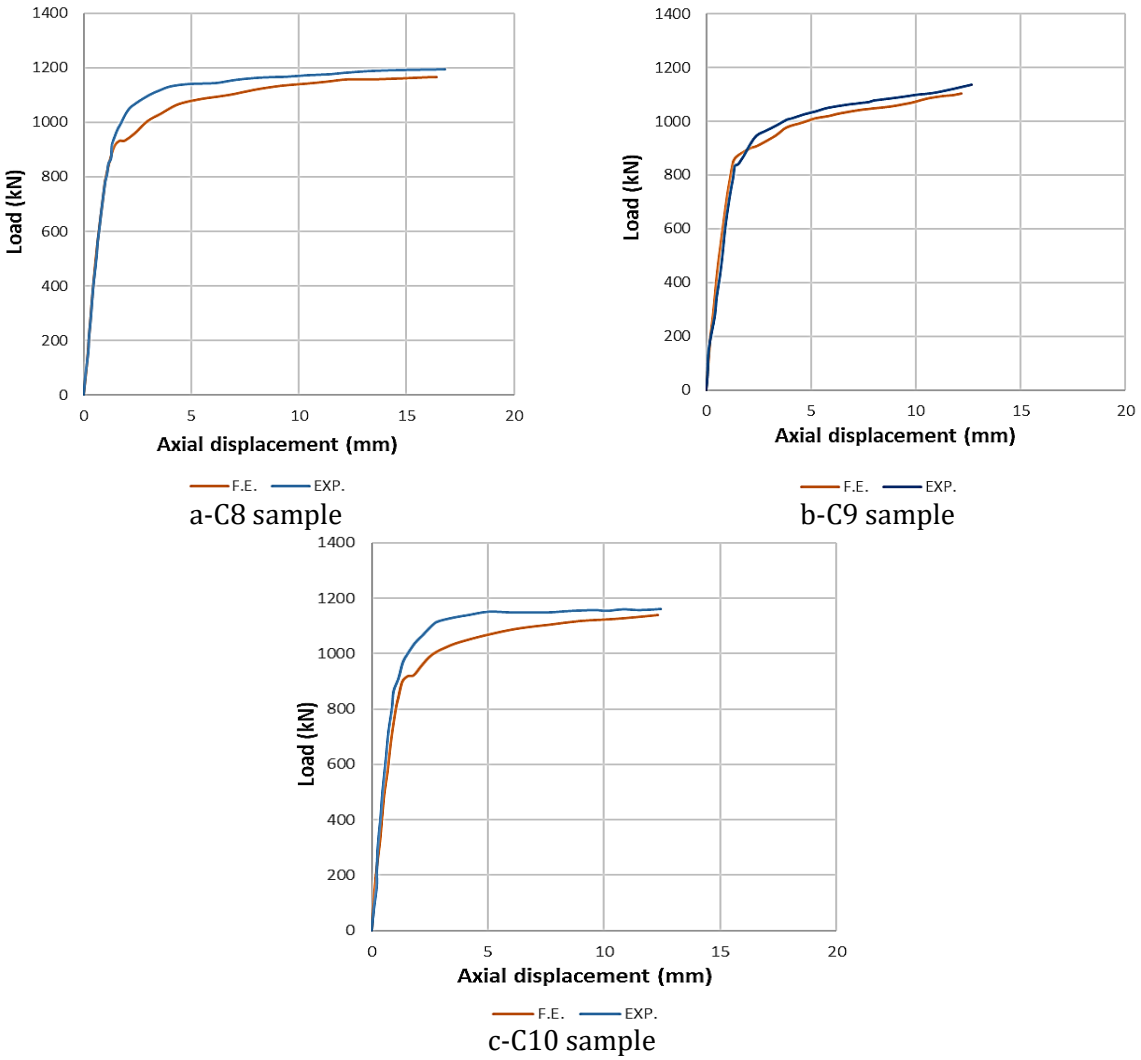


Fig. 6. Analyzing the load against the axial displacement both numerically and experimentally

6. Numerical Parametric Study

Following the prior verification of the finite element (FE) assessment for the experimental findings acquired in this research, an extensive parametric analysis was conducted utilizing the numerical model with 10 circular CFST column configurations as presented in Table 5. The investigation parameters are:

- Concrete skin: single-skin (outer tube only) or double-skin (outer and inner tube).
- Vertical spacing of shear connectors (bolts) (50, 100, or 200mm).

- Thickness of outer tube (2, 4, or 6mm).

These values were selected based on previous research. Recognizing that all samples possess the same other properties such as: Total height of column =1245mm, outer tube diameter = 225mm, inner tube diameter = 50mm, inner tube thickness = 2.8mm. The length of bolt=500mm and the diameter of bolt =9.5mm. The testing method for all samples was carried out by applying an axial central load to the concrete and steel tubes. The compressive strength of concrete here fc'=32MPa and splitting tensile strength= 3.2MPa. Table 6 shows the properties of steel tube and bolts.

Table 5. Information of the case study CFST columns

column name	Skin type	Thickness of outer tube (mm)	Vertical spacing of shear connectors (mm)
DSC4	Double	4	-
DSC4-50	Double	4	50
DSC4-100	Double	4	100
DSC4-200	Double	4	200
SSC4	Single	4	-
SSC6	Single	6	-
SSC2	Single	2	-
SSC4-50	Single	4	50
SSC4-100	Single	4	100
SSC4-200	Single	4	200

Table 6. Properties of the steel tube and bolts

Material	Elongation percentage (%)	Fy (MPa)	Fu (MPa)	Ec (MPa)
Steel of tube	11	350	500	200000
Bolts	10.8	768.6	791.3	210200

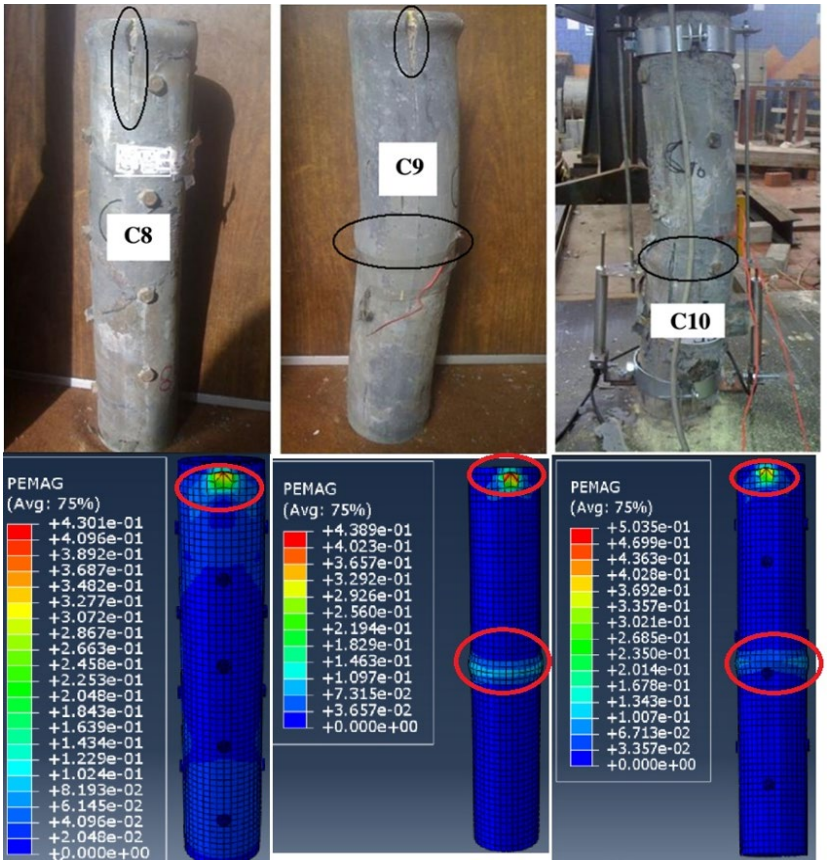
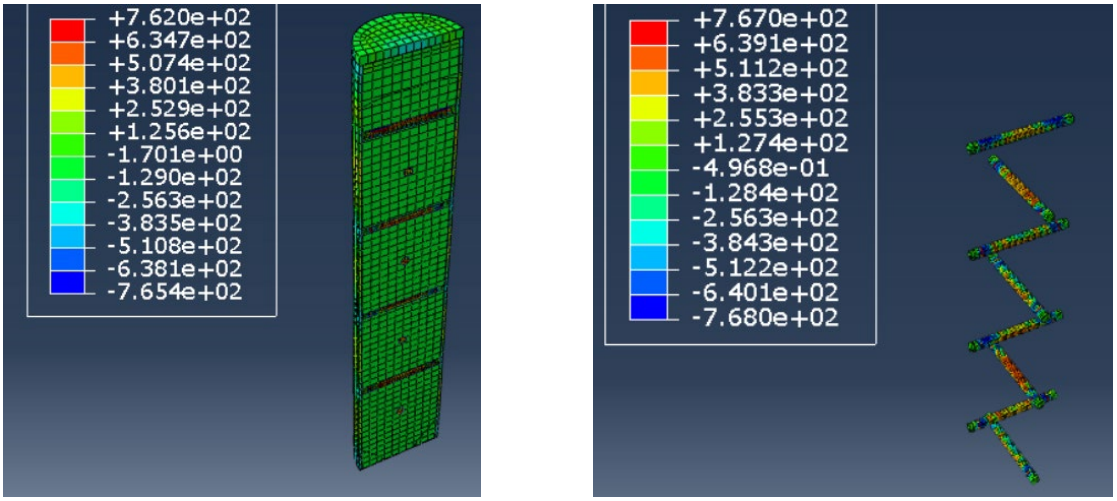
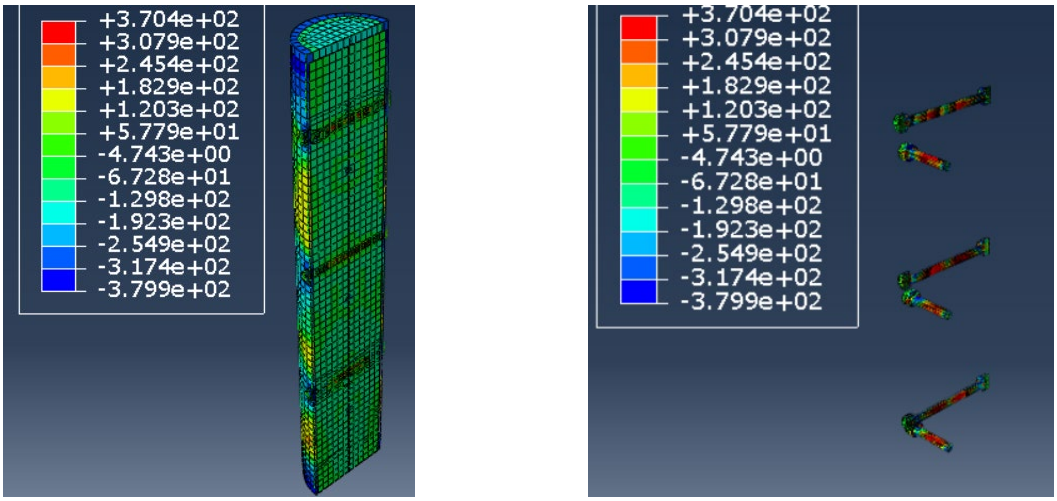


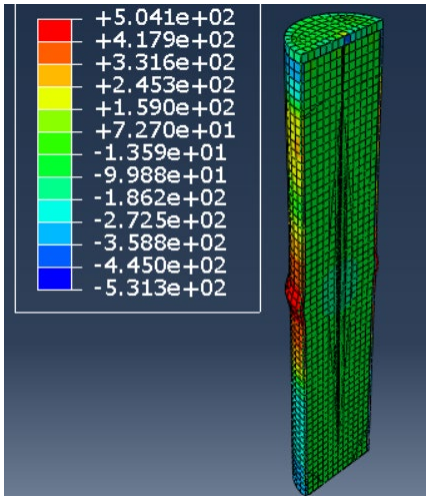
Fig. 7. Failure mode both numerically and experimentally



a-C8 column



b-C10 column

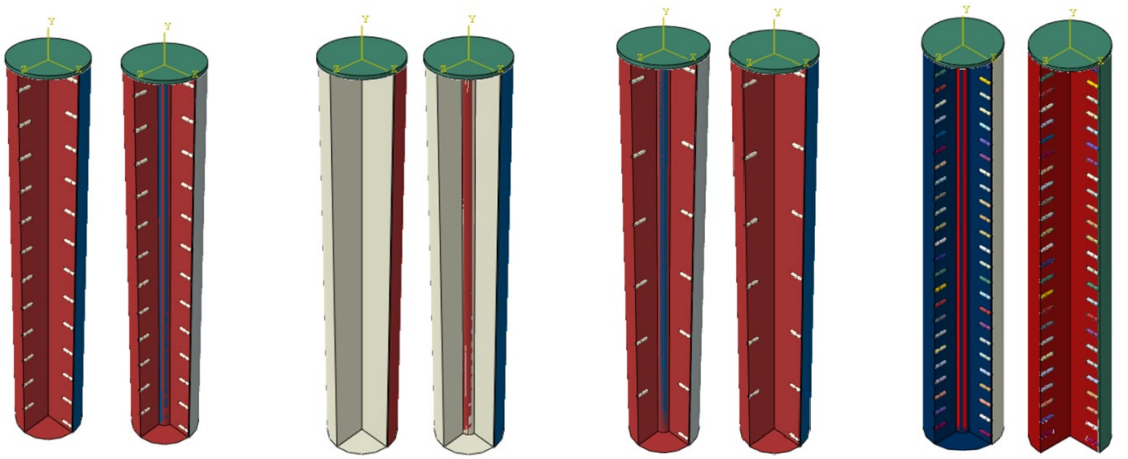


c-C9 column

Fig. 8. Stress distribution in CFST components (MPa)

6.1 Effect of the Concrete Skin (Single or Double)

Four specimens were single-skin concrete (CFST columns with outer tube only): no shear connectors and with shear connectors spacing 50, 100, and 200mm. In contrast there are four specimens that are exactly the same, but of the double-skin type (CFST columns with outer and inner tube). Therefore, 8 specimens were used here to study the impact of the concrete skin type. See Figure 9.



a- Spacing 100 mm | b- No shear connectors | c- Spacing 200 mm | d- Spacing 50 mm

Fig. 9. CFST columns of the concrete skin type

6.1.1 Load vs. Axial Displacement Relation

The influence of the concrete skin type on the load vs axial displacement relationship for the 4 groups is displayed in Figure 10. Based on load vs. axial displacement relationships, it is clear that for CFST columns without shear connectors, the stiffness was similar at the linear part for both columns, but in the non-linear part, the column with double skin gave a greater stiffness. While for CFST columns with shear connectors, approximately the column with double skin gave a greater stiffness in all parts of the curves except for a small part in the middle, this may be due to the additional confinement effect provided by the inner tube. The DSC4-200 specimen deviates from the others; this may be due to the studs losing interaction with the concrete.

6.1.2 Ultimate Load

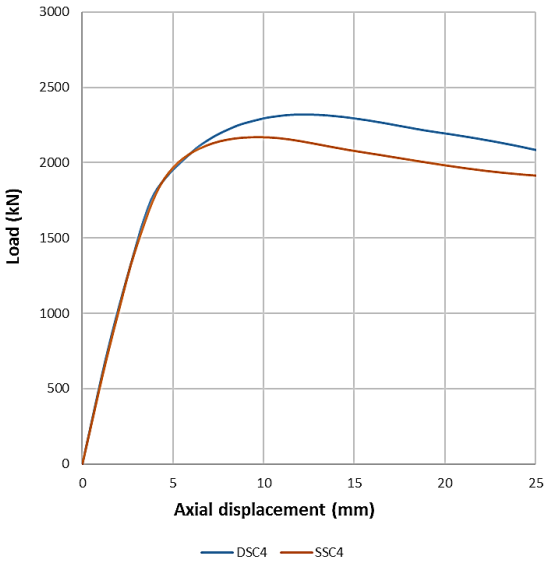
Table 7 illustrates that the percentage decrease in the ultimate load for a single-skin column, in comparison to an analogous double-skin column, was 6.5, 4.8, 6.6, and 5.1% for the column devoid of shear connections, the column with shear connectors spacing of 50, 100, and 200mm, respectively. All double-skin columns have a superior load capacity compared to their single-skin counterparts, regardless of the presence of shear connections. This may result from the selected dimensions of the samples and the inclusion of the internal steel tube, which enhances the column's load-bearing capability.

Table 7. Impact of the concrete skin type on the failure load

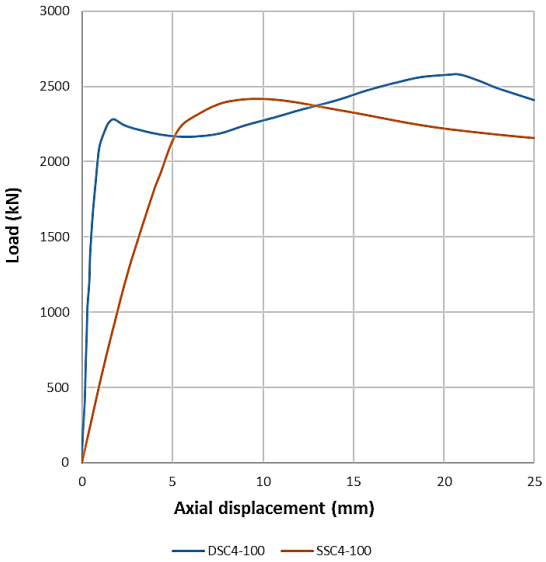
column name	Failure Load (Pu) (kN)	Axial disp. at failure load (Δu) (mm)	% Decrease in Pu with respect to Ref.
DSC4	2319	12.2	Ref.
SSC4	2169	10.4	6.5
DSC4-50	2650	16.5	Ref.
SSC4-50	2523	10.7	4.8
DSC4-100	2585	20.5	Ref.
SSC4-100	2414	10.8	6.6
DSC4-200	2335	21.6	Ref.
SSC4-200	2217	10.8	5.1

6.2 Impact of the Thickness of Outer Steel Tube

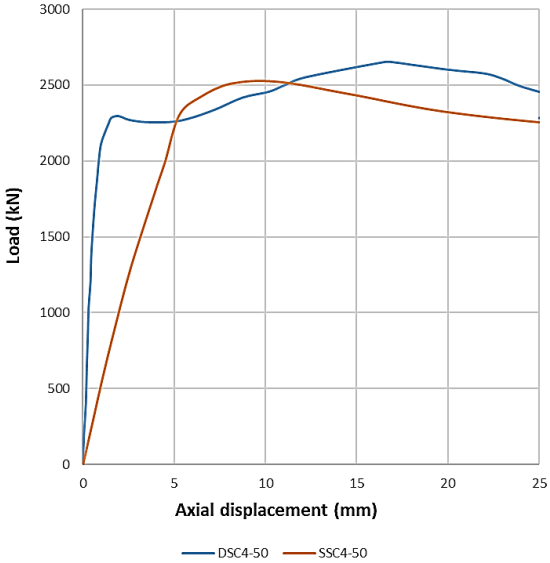
Three specimens were used to demonstrate the impact of the thickness of outer steel tube (2, 4, or 6mm) on the structural performance of single skin CFST columns without bolts.



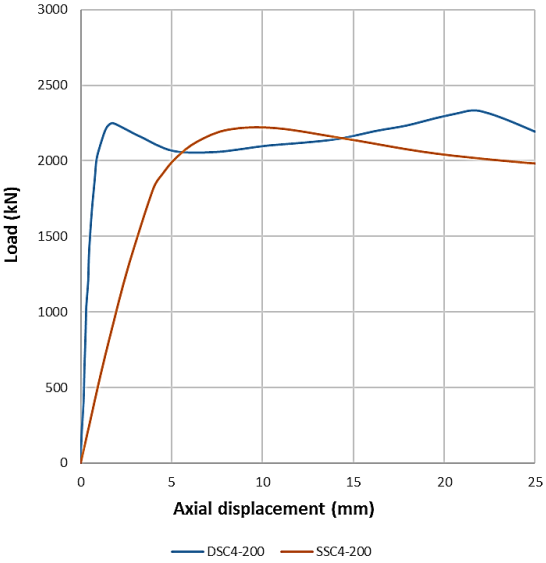
a- Without shear connectors group



b- Shear connectors spacing of 100mm group



c- Shear connectors spacing of 50mm group



d- Shear connectors spacing of 200mm group

Fig. 10. Effect of the concrete skin type on load vs axial displacement relationship

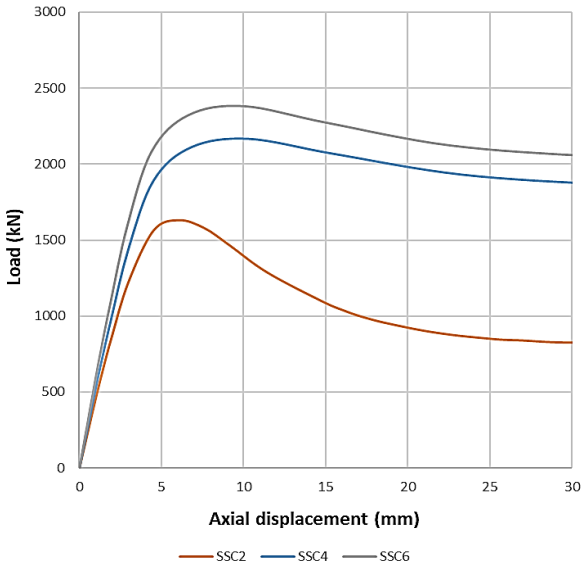


Fig. 11. Effect of the outer tube thickness on load vs axial displacement relationship

6.2.1 Load vs. Axial Displacement Relationship

Figure 11 shows that the outer tube thickness does not significantly affect the linear part of the curves, but after the non-linear part begins and reaches the failure stage, the outer tube thickness is directly proportional to the column stiffness. A reduction in the outer pipe's wall thickness leads to local buckling, resulting in rapid failure and compromising load-bearing capacity.

6.2.2 Ultimate Load

Table 8 shows that raising the thickness of the outer tube results in an enhancement of ultimate strength by 32.8 and 46 % for the column with outer tube thicknesses of 4.0 and 6.0 mm, respectively, compared to the column with the outer tube thickness of 2 mm. The thickness of the outer tube is proportional to the column's ultimate load. The significant improvement in the column's load-bearing capacity—relative to the minor cost difference resulting from the increased pipe thickness—makes it worthwhile.

Table 8. Impact of the thickness of outer steel tube on the failure load

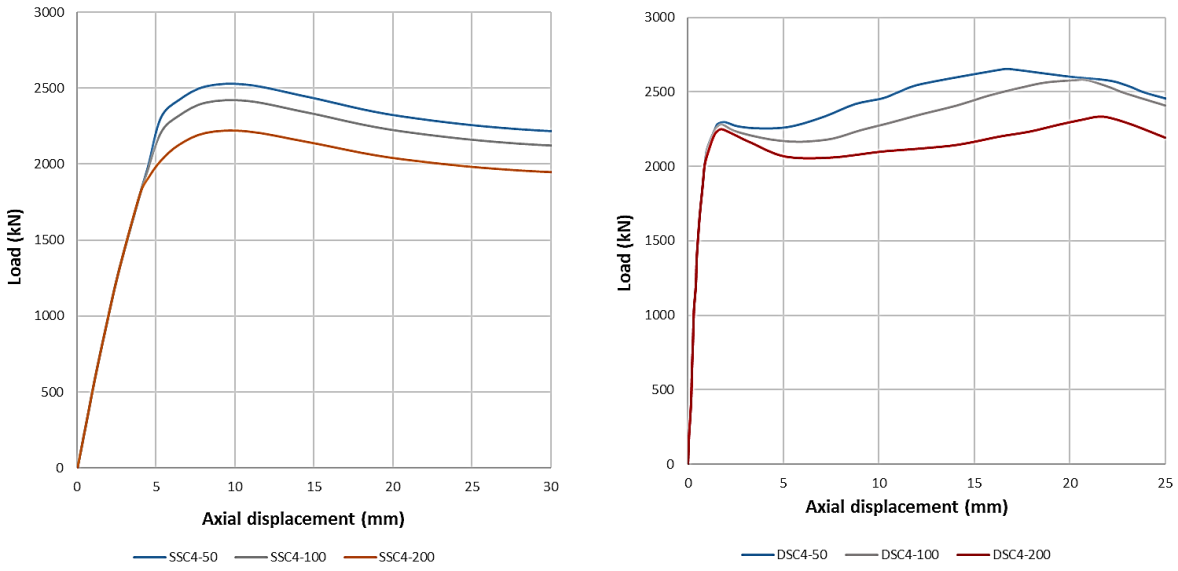
column name	Failure Load (Pu) (kN)	Axial disp. at failure load (Δu) (mm)	% Increase in Pu with respect to Ref.
SSC2	1633	6.1	Ref.
SSC4	2169	10.4	32.8
SSC6	2384	10	46

6.3 Effect of The Vertical Spacing of Shear Connectors

Two groups were made here, where the first group included three double-skin specimens equipped with shear connectors at spacing of 50, 100, and 200 mm, while the second group included three single-skin models equipped with shear connectors at spacing of 50, 100, and 200 mm.

6.3.1 Load – Axial Displacement Relation

Figure 12 shows that the spacing of bolts does not significantly affect the linear part of the curves, but after the non-linear part begins and reaches the failure stage, the spacing is inversely proportional to the column stiffness. In part b, the DSC4-200 specimen deviates from the others; this may be due to the studs losing interaction with the concrete.



a- Single skin b- Double skin

Fig. 12. Effect of shear connector spacing on load-displacement behavior

6.3.2 Ultimate Load

Table 9 shows that decreasing the vertical spacing of shear connectors results in an enhancement of ultimate strength by 8.9, and 13.8 % for the single skin columns with spacing of 100 and 50 mm,

respectively, compared to the single skin column with spacing of 200 mm, and by 10.7, and 13.5 for the double skin columns with spacing of 100 and 50 mm, respectively, compared to the double skin column with spacing of 200 mm. The vertical spacing of shear connectors is inversely proportional to the column's ultimate load.

Table 9. Influence of the vertical spacing of shear connectors on the failure load

column name	Failure Load (Pu) (kN)	Axial disp. at failure load (Δu) (mm)	% Increase in Pu with respect to Ref.
SSC4-200	2217	10.8	Ref.
SSC4-100	2414	10.8	8.9
SSC4-50	2523	10.7	13.8
DSC4-200	2335	21.6	Ref.
DSC4-100	2585	20.5	10.7
DSC4-50	2650	16.5	13.5

7. Conclusions

- Results from experiments and finite element models showed a high degree of agreement when it came to the ultimate load and axial displacement, with the mean and coefficient of variation of (Pu) FE/(Pu) EXP being 0.976 and 0.54%, respectively, for failure loads, whereas for the axial displacement (Δu FE / Δu EXP) they were 0.975 and 1.36%, respectively.
- The ultimate load reduction for a single-skin column, relative to a comparable double-skin column, was 6.5%, 4.8%, 6.6%, and 5.1% for the column without shear connections and those with shear connector spacings of 50, 100, and 200mm, respectively. All double-skin columns exhibit enhanced load-bearing capability in comparison to single-skin variants, irrespective of shear connection inclusion. This might stem from the chosen size of the samples and the incorporation of the internal steel tube, which bolsters the column's load-bearing capacity.
- Increasing the outer tube's thickness leads to an improvement in ultimate strength by 32.8% and 46% for columns with outer tube thicknesses of 4.0 mm and 6.0 mm, respectively, as compared to the column with a 2 mm outer tube thickness. The outer tube's thickness correlates with the column's maximum load capacity.
- Reducing the vertical spacing of shear connectors leads to an increase in ultimate strength of 8.9% and 13.8% for single skin columns with spacings of 100 mm and 50 mm, respectively, in comparison to the single skin column with a spacing of 200 mm, and by 10.7% and 13.5% for double skin columns with spacings of 100 mm and 50 mm, respectively, when compared to the double skin column with a spacing of 200 mm. The vertical spacing of shear connections is inversely related to the ultimate load of the column.
- From the previous conclusions, it can be concluded that, in terms of economic and structural performance, 4 mm outer tube thickness and 100 mm stud spacing were found to be the most efficient configuration" should be added.
- The primary constraints of numerical models for Concrete-Filled Steel Tubular (CFST) columns pertain to difficulties in precisely representing intricate material interactions, such as the simulation of bond-slip behavior and the detachment between the internal concrete core and the external steel tube, as well as modelling cracking and damage, and boundary conditions.
- As a future study, we propose to study the structural behavior of CFST columns with shear studs under the effect of cyclic loading or impact loading.

References

[1] Lu Y, Li N, Li S, Liang H. Behavior of steel fiber reinforced concrete-filled steel tube columns under axial compression. Construction and Building Materials. 2015;95:74-85. https://doi.org/10.1016/j.conbuildmat.2015.07.114

[2] Isleem HF, Chukka NDKR, Bahrami A, Oyebisi S, Kumar R, Qiong T. Nonlinear finite element and analytical modelling of reinforced concrete filled steel tube columns under axial compression loading. Results in Engineering. 2023;19:101341. https://doi.org/10.1016/j.rineng.2023.101341

[3] Sangeetha P, Prithvi R, Kumaran VA, Murali B, Yaashika M. Structural behavior of deficient hollow steel columns strengthened using GFRP. Res Eng Struct Mater. 2025;11(2):1-17. https://doi.org/10.17515/resm2025-541st1121rs

[4] Kim SE, Papazafeiropoulos G, Truong VH, Nguyen PC, Kong Z, Duong NT, et al. Finite element simulation of normal-strength CFDST members with shear connectors under bending loading. Engineering Structures. 2021;238:112011. https://doi.org/10.1016/j.engstruct.2021.112011

[5] Abdulkareem BF, Izzet AF. Post fire residual concrete and steel reinforcement properties. In: IOP Conference Series: Earth and Environmental Science. IOP Publishing; 2021. p. 012058. https://doi.org/10.1088/1755-1315/856/1/012058

[6] Chen CC, Wu PD, Zhang GY. New type of shear connector for square concrete-filled tubular columns. Advances in Structural Engineering. 2022;25(12):2467-2482. https://doi.org/10.1177/13694332221098865

[7] Almamoori AHN, Naser FH, Dhahir MK. Effect of section shape on the behaviour of thin-walled steel columns filled with light weight aggregate concrete: Experimental investigation. Case Studies in Construction Materials. 2020;13:e00356. https://doi.org/10.1016/j.cscm.2020.e00356

[8] Cao B, et al. Axial compression performance of precast circular semi-continuous concrete-filled steel tube columns: Finite element analysis and theoretical modeling. Buildings. 2023;13(2):284. https://doi.org/10.3390/buildings13020284

[9] Zhang S, et al. Experimental and theoretical study of concrete-filled steel tube columns strengthened by FRP/steel strips under axial compression. International Journal of Concrete Structures and Materials. 2023;17(1):1. https://doi.org/10.1186/s40069-022-00556-2

[10] Essopjee Y, Dundu M. Performance of concrete-filled double-skin circular tubes in compression. Composite Structures. 2015;133:1276-1283. https://doi.org/10.1016/j.compstruct.2015.08.033

[11] He K, et al. Compressive performance of eccentrically double-cell concrete-filled circular steel tubular columns. Journal of Constructional Steel Research. 2024;217:108639. https://doi.org/10.1016/j.jcsr.2024.108639

[12] Qiao Q, Zhang X, Hu J. A study on shear connectors of square concrete filled steel tubes. International Journal of Structural and Civil Engineering Research. 2015;4(3):254-258. https://doi.org/10.18178/ijscer.4.3.254-258

[13] Qiao Q, Zhang W, Qian Z, Cao W, Liu W. Experimental study on mechanical behavior of shear connectors of square concrete filled steel tube. Applied Sciences. 2017;7(8):818-828. https://doi.org/10.3390/app7080818

[14] Sarir P, et al. Iterative finite element analysis of concrete-filled steel tube columns subjected to axial compression. Buildings. 2022;12(12):2071. https://doi.org/10.3390/buildings12122071

[15] Zhang Y, et al. Investigation on shear behavior of longitudinal-plate shear connector in concrete-filled steel tube. Thin-Walled Structures. 2026:114672. https://doi.org/10.1016/j.tws.2026.114672

[16] Habib MA, et al. Experimental study on prefabricated CFST columns with bolt-coupler baseplate connections under compression. Thin-Walled Structures. 2026;221:114465. https://doi.org/10.1016/j.tws.2025.114465

[17] Younes SM, Ramadan HM, Mourad SA. Stiffening of short small-size circular composite steel-concrete columns with shear connectors. Journal of Advanced Research. 2016;7(3):525-538. https://doi.org/10.1016/j.jare.2015.08.001

[18] Dassault Systèmes. Abaqus 2022 user assistance user's manual, Ver. 2022. Hibbitt, Karlson and Sorensen, Inc.; 2022.

[19] Majumder S, Saha S. Shear behaviour of RC beams strengthened using geosynthetic materials by external and internal confinement. Structures. 2021:1665-1678. https://doi.org/10.1016/j.istruc.2021.03.107